

Transient performance of alternatively fueled internal combustion engines for naval applications

Ir. J Vollbrandt^{a*}, Dr. ir. R D Geertsma, CEng, FIMarEST^b, Dr. A Coraddu, MSc, CEng, MIMarEST^a

^aDelft University of Technology, The Netherlands; ^bNetherlands Defence Academy, The Netherlands

*Corresponding author. Email: j.vollbrandt@tudelft.nl

Synopsis

While navies worldwide aim to reduce their exhaust gas emissions, fossil fuel dependency and signatures, engines on alternative fuels, such as natural gas and methanol, are limited by a lower dynamic load acceptance than diesel engines. This load acceptance is crucially important for naval vessels, both for high maneuverability and for handling pulsed power loads for rail-guns and directed energy weapons. Previous research into the dynamic response of natural gas engines focused on detailed in-cylinder combustion models to predict knock. These OD/1D simulation models rely on extensive data to calibrate the combustion model, which is generally unavailable to naval engineers and scientists designing a propulsion or energy system. Additionally, these simulation models require a significant amount of computational power and rarely run in real-time. For the evaluation of the dynamic behaviour of such engines during actual manoeuvres and for their use in control oriented modelling approaches, real-time dynamic models are required for natural gas and methanol engines. This study investigates the dynamic response of a spark ignited gas engine with single point fuel injection using a Mean Value First Principle (MVFP) engine model based on the filling and emptying approach and turbocharger performance maps derived from limited data and measurements. For three relevant military scenarios we demonstrate that a gas engine with single point fuel injection driving a generator can comply with the requirements of NATO STANAG 1008 for Quality Power Supply. Furthermore, during these scenarios, transient performance of the gas engine is limited by the inertia of the air path rather than engine knocking.

Keywords: Modeling and simulation; Mean value first principle model; Transient performance; Alternative fuels; Thermal loading; Knock probability

1 Introduction

Navies worldwide are exploring the use of alternative fuels for their vessels, aiming to cut down greenhouse gas emissions, reduce signatures and lessen their reliance on fossil fuels [1]. In the long run, fuel cells and batteries might provide zero-emission power systems for ships, but currently they cannot provide sufficient energy and power for naval vessels due to their limited energy density. Therefore, in the short and medium term, navies can reduce their fossil fuel dependency and retain operational flexibility by applying alternative fuels, that can be produced sustainably. Since the requirements on power density are strict, many navy vessels rely on gas turbine and high speed diesel engines running on F76 marine diesel fuel and replacements for F76 in these conventional propulsion systems are consequently favoured. Methanol is particularly interesting due to the lower toxicity, a liquid state at standard conditions and a sustainable production that can be easily scaled up compared to other alternative fuels [2, 3]. Introducing low reactivity fuels, including most alternative fuels like natural gas or alcohols, however, results in reduced load acceptance of internal combustion engines and specifically piston engines [4, 5] which consequently might not meet the stringent naval requirements for dynamic load capacity. Traditionally, naval vessels require a high dynamic load capacity on the propulsion engines for high maneuverability [6]. Moreover, with recent developments in naval rail guns and directed energy weapons the required dynamic load capacity within the electric power generation is increasing as well [7]. To solve this dilemma, engineers and scientists need to investigate and improve the transient behaviour of piston engines running on low reactivity fuels.

Currently, two ignition principles are considered for the combustion of low reactivity fuel. Firstly, the fuel can be ignited by a spark plug according to the Otto cycle. Secondly, the fuel can be ignited by compression ignition (CI) using the diesel principle by injecting a small amount of high reactivity fuel to start the combustion. Advantage of the latter is a higher efficiency and fuel flexibility but at the cost of a more complex fuel handling

Authors' Biographies

Jasper Vollbrandt currently is PhD researcher at Delft University of Technology and Netherlands Defence Academy on dynamic behaviour of alternately fueled internal combustion engines. He has previously worked on ship propulsion systems for the Command Materiel and IT of the Dutch Ministry of Defense and as a project engineer hydraulics for TATA Steel Netherlands.

Cdr (E) Rinze Geertsma currently is assistant professor at the Netherlands Defence Academy and research fellow at Delft University of Technology with a research interest in sustainable and maintainable energy systems for ships. He previously has been Marine Engineering Officer of HNLMS de Ruyter and HNLMS Tromp. Earlier experience include system and project engineering and innovation roles.

Prof. Andrea Coraddu is an Associate in the Department of Maritime and Transport Technology of Delft University of Technology. In 2012 he was awarded a Laurea and a PhD in Naval Architecture and Marine Engineering at the University of Genoa. His research lies at the forefront of the maritime energy transition, delving into the topology design, performance optimization, and control of hybrid and full electric marine energy systems.

system and a higher control effort [8]. Dual-fuel CI technology for marine engines is investigated extensively and several dual-fuel gas engines are commercially available. Research on marine spark ignited engines running on natural gas or methanol however is scarce, despite the simpler fuel handling and control. Relying on spark-ignition could offer advantages such as better control and lower NO_x emissions for smaller high speed engines suited for naval applications [9, 10].

Investigating and evaluating dynamic behaviour of engines, propulsion plants and their corresponding control approach is extensively supported by simulation models. The model approach can help identify thermodynamic engine limitations, for example due to excessive temperatures in the cylinder [11], and limitations in the gas path due to turbocharger lag [12] or improve the system control strategy of the entire propulsion plant [13, 14]. Detailed computational fluid dynamics (CFD) engine models are able to estimate pressure and heat release rate of the in-cylinder process running on different blends of fuel with high accuracy [15, 16] and can predict emissions as well [17, 18]. However, these models can rarely run in real-time and are therefore not suited for the scope of this paper. Computational less expensive 1D/0D crank-angle models sacrifice accuracy of the in-cylinder process by predicting the released heat during combustion with a Wiebe function [19]. Improvements in accuracy are achieved by implementing several Wiebe functions to describe separate combustion phases of a diesel fuel [20, 21], natural gas [22] or a mixture of fuels [23, 24]. However, for dynamic and control oriented purposes simplifying the implementation of the in-cylinder process with a mean-value approach can result in sufficiently accurate results [25, 26], especially when considering the 6-point Seiliger process [22]. More important for a dynamic model is an accurate prediction of the gas path dynamics [27, 28]. Marine engine models can predict gas path dynamics with several approaches, but their application is so far limited to compression ignition running either on diesel fuel [12, 29, 30] or on diesel and gas as dual fuel application [31, 32]. Tavakoli et al [33] investigate a marine natural gas spark ignited engine with port fuel injection and eliminate the engine speed control by the throttle valve. Speed control by the throttle valve and the dynamics of the throttled mass flow are investigated extensively for automotive using gasoline as a fuel [34–36].

The aim of this paper is to propose a novel real-time modelling approach for a marine spark ignition gas engine with single point fuel injection and to evaluate the dynamic performance of low reactivity fuel combustion engines. A novel method is introduced to obtain the Seiliger parameters by calibrating and evaluating the in-cylinder process with the indicated work, maximum cylinder pressure and the pressure before opening of the exhaust valve. Furthermore, a novel method for predicting the gas path dynamics of a marine spark ignition engine is introduced consisting of a three volume element approach for engines with throttle valve control and the corresponding throttle valve controller and dynamics. The model incorporates a method to derive performance maps for the compressor and turbine, considering these maps are not always available. The model is used to investigate several load profiles and draw conclusions on the drivers and limitations of transient performance for these types of engines.

2 Theoretical Framework

The proposed engine simulation model is a generic model of a marine high-speed, 4-stroke, spark-ignited gas engine with single point of injection driving a generator at constant speed and the corresponding engine controller according to the schematic layout in Figure 1. The proposed MVFP engine model relies on the 6-point Seiliger cycle [37] to estimate pressure, temperature and indicated work of the closed in-cylinder process. This in-cylinder process with corresponding heat release functions are implemented according to Geertsma et al. [38] and Schulten [39]. The block diagram of the simulation model is illustrated in Figure 2.

The air and exhaust path dynamics are estimated with the filling and emptying approach [40] combined with

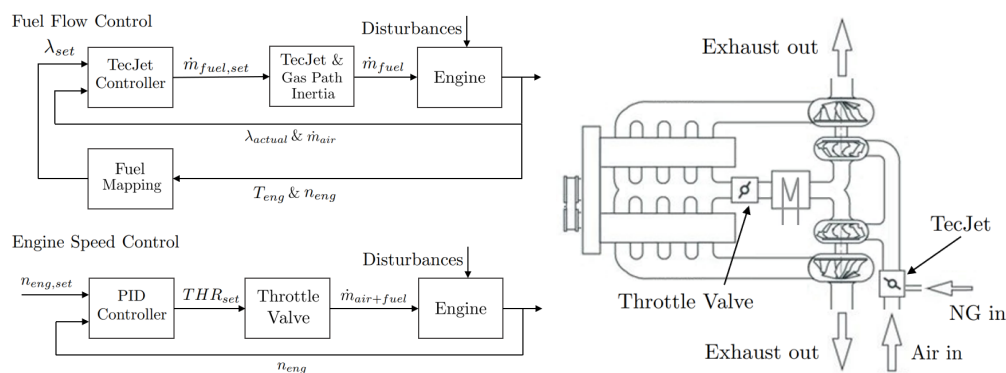


Figure 1: Schematic layout of the engine and controller

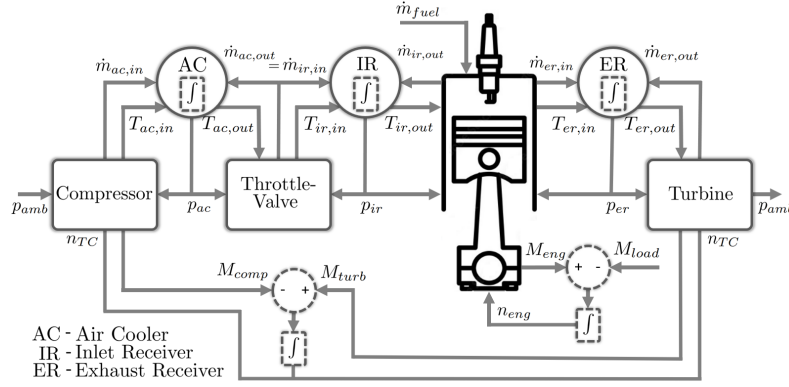


Figure 2: Block diagram of the proposed simulation model showing the volume elements involved in the gas exchange process [12].

a map-based turbocharger model. In Figure 2, the volume elements are represented by circles and the resistance elements by rectangles. To reduce the amount of volume elements, and thus the amount of differential equations, volume elements will be combined if possible to reduce computational cost. For the air path, two volume elements are necessary to determine the pressure before and after the throttle valve. The throttle valve is implemented as a throttle valve with variable throat area according to Heywood [19]. The necessary volume element after the compressor will be combined with the volume element before the throttle valve into a single volume element of the air cooler. Likewise, the volume element before the cylinder can be combined with the volume element after the throttle valve into a single volume element for the inlet receiver. For the exhaust path, a single volume element is implemented, combining the volume element needed after the cylinder and before the turbine.

The turbocharger performance model consists of the compressor and turbine elements that are coupled by the rotational speed of the turbocharger shaft. The delivered mass flow and isentropic efficiency of the compressor are obtained by linear interpolation from the compressor performance map. With the mass flow, isentropic efficiency and rotational speed of the turbocharger, torque delivered by the turbine and consumed by the compressor are determined. The shaft speed is determined with the equation of motion, as follows:

$$\frac{dn_{TC}}{dt} = \frac{\eta_{m,TC}(\tau_{turb} - \tau_{comp})}{2\pi J_{TC}}, \quad (1)$$

where τ_{turb} is the delivered torque of the turbine, τ_{comp} is the consumed torque of the compressor, $\eta_{m,TC}$ is the mechanical efficiency of the turbocharger and J_{TC} is the turbochargers polar moment of inertia. The performance map for the compressor is derived using the method described by Casey and Robinson [41]. For deriving the turbine map, the method proposed by Jensen [42] is implemented as described by Moraal and Kolmanovsky [43]. Model assumptions for the implemented methods are given in Table 1. Technical specifications are derived from the manufacturer data [44, 45]. The resulting compressor performance map and efficiency plot are given in Figure 3.

In contrast to modern diesel engines with direct injection of fuel, the engine speed of the gas engine is controlled with the throttle valve and the fuel supply is controlled by a gas valve. The throttle valve forms a controllable restriction for the mass flow of gas from the compressor to the inlet receiver. Opening of the throttle valve decreases the flow resistance of the gas, resulting in a higher mass flow to the inlet receiver and a higher inlet receiver pressure. A PID controller is implemented for the translation of the engine speed set point to the throttle valve set point. The TecJet gas valve controls the mass flow of natural gas to be mixed with fresh air before the compressor. Set points for the gas valve are determined by the TecJet controller based on the desired and actual air-to-fuel ratio

Table 1: Design point parameters Garrett TW6146

| Compressor parameter | Value | Turbine parameter | Value |
|-------------------------------|-------------------------|----------------------------|-------|
| Turbocharger shaft speed | 81500rpm | Turbine expansion ratio | 1.77 |
| Compressor pressure ratio | 1.95 | Temperature turbine inlet | 560°C |
| Temperature compressor inlet | 40°C | Temperature turbine outlet | 409°C |
| Temperature compressor outlet | 136°C | | |
| Compressor volume flow | 0.3382m ³ /s | | |

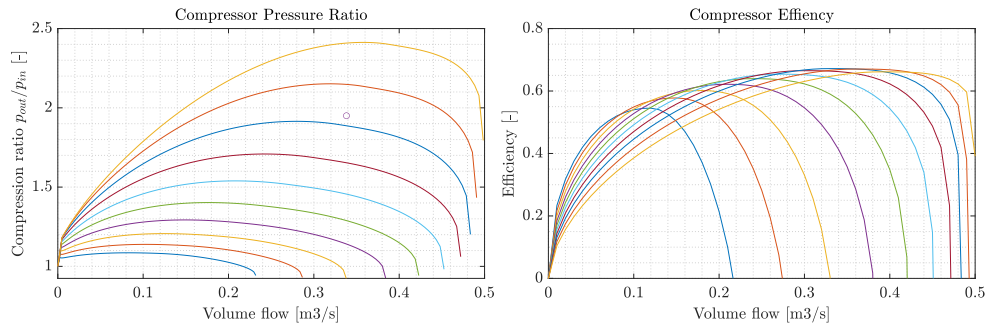


Figure 3: Compressor performance plots showing the pressure ratio on the left and the efficiency on the right for compressor tip speeds ranging from $0.4 - 1.3Ma$

and the mass flow of fresh air. The desired air-to-fuel ratio is retrieved by the engine controller from the fuel map prescribing the desired air-to-fuel ratio for every torque and speed setting of the engine.

3 Case Study

For the case study, the Caterpillar 3508A high-speed, 4-stroke, spark-ignited gas engine was selected. In the experimental setup this engine drives a generator at constant speed. The engine parameters are given in Table 2. This engine is currently running on natural gas (NG) with all fuel injected before the compressor but has run on methanol and different blends of NG with hydrogen in the past [46, 47]. Since it is also available for marine propulsion applications, the engine is a good representative in size and power for an auxiliary diesel generator on naval vessels such as frigates and patrol vessels or as a main diesel generator on smaller support vessels such as the hydrographic survey vessels of the Royal Netherlands Navy [48, 49].

3.1 Data acquisition

The experimental setup is operated by the engine laboratory of the Netherlands Defense Academy in Den Helder. Pressure and temperature sensors located in the gas path are read-out with a sample time of 200ms by a coupled National Instruments cRIO-9057. The turbocharger speed is assessed with an optic sensor directed at the turbocharger shaft. The in-cylinder pressure is obtained with the standard piezoresistive pressure sensors connected to a Kistler KiBox and is crank angle resolved with a resolution of 0.1° . An overview of the used sensors is given in Table 3.

3.2 Model calibration

To calibrate the developed MVFP engine model in steady state operating points and during transient operation, a measurement run the Caterpillar 3508A gas engine was executed on idle, 20%, 50%, 75% and 90% of the MCR load. Unfortunately, 100% load was not possible and 90% load was possible on a slightly lower engine speed due to an insufficient NG grid pressure. Additional engine parameters have been obtained from the operating and maintenance manual [44] and the engine specifications leaflet [50]. The implemented components, described in Section 2,

Table 2: Engine parameters Caterpillar 3508B

| Basic parameters | Value | Charge air parameters | Value |
|------------------------|---------------------------------------|-------------------------|----------------|
| Number of cylinders | 8 | Turbocharger type | Garrett TW6146 |
| Rated speed | 1500 rpm | TC quantity | 2 |
| Cylinder arrangement | 60° V | TC configuration | Parallel |
| Rated power | 500 kW | Max charge air pressure | 2.2 bar |
| Bore | 170 mm | | |
| Stroke | 190 mm | | |
| Displacement | 34.5 L | | |
| Compression ratio | 12:1 | | |
| Fuel supply parameters | | | |
| Fuel type | Low-calorific natural gas | | |
| Injection method | Single point injection(SPI) before TC | | |
| Ignition method | Spark ignited (SI) | | |

Table 3: Sensor List

| Feature | Manufacturer | Type |
|--|--------------------|------------|
| Mass flow inlet air \dot{m}_{in} | Sierra Instruments | 640i VT |
| Temperature inlet air T_{in} | Sierra Instruments | 640i VT |
| Mass flow fuel \dot{m}_{fuel} | Bronkhorst | F-106 CI |
| Pressure before compressor $p_{comp,in}$ | GE Druck | PTX 1400 |
| Pressure after compressor $p_{comp,out}$ | GE Druck | PTX 5072 |
| Pressure before throttle p_0 | Jumo | dTRANS p30 |
| Pressure inlet receiver p_{ir} | Jumo | dTRANS p30 |
| Pressure before turbine $p_{turb,in}$ | GE Druck | PTX 5072 |
| Pressure after turbine $p_{turb,out}$ | GE Druck | PTX 1400 |

have been calibrated individually by using the obtained measurement data. The calibrated components have been integrated into the complete engine model and the model was validated subsequently. All model parameters are summarized in Table 5, Appendix A.

For validation, a measurement run on the experimental set up has been executed on constant engine speed with load steps increasing from 16% to 30%, 60%, and 80% and decreasing from 80% to 50% and 20% of the MCR load, at different operating points than for calibration. The results show that the model captures the turbocharger and gas path dynamics well above 20% and the corresponding transient phases, see Figures 4 and 5. Results for steady state conditions are within 5% for most of the measured values. Deviations during transient phases are larger but the behaviour of engine parameters is captured well. At loads below 20% the model accuracy decreases for the static operating points and the transient behaviour is captured less accurately. The simulation results of the validation have been obtained with MATLAB Simulink R2022b running on a Intel Core i7 – 1265U processor and 16 GB RAM. The required time to run the simulated time of 420s was 5.4s. The current set up is able to run the model about 77 times faster than real-time.

4 Investigation of typical dynamic naval load profiles

A series of simulation experiments with highly varying and pulsed loads were designed and executed to examine the transient performance of the spark-ignited gas engine with single point injection. During these simulation experiments the engine is assumed to drive a constant speed generator at 1500rpm with varying load profile. All other engine parameters are held constant according to the calibration parameters of the case study. The results of these experiments provide insight in the transient behaviour of single point injection spark ignition engines with standard control methods.

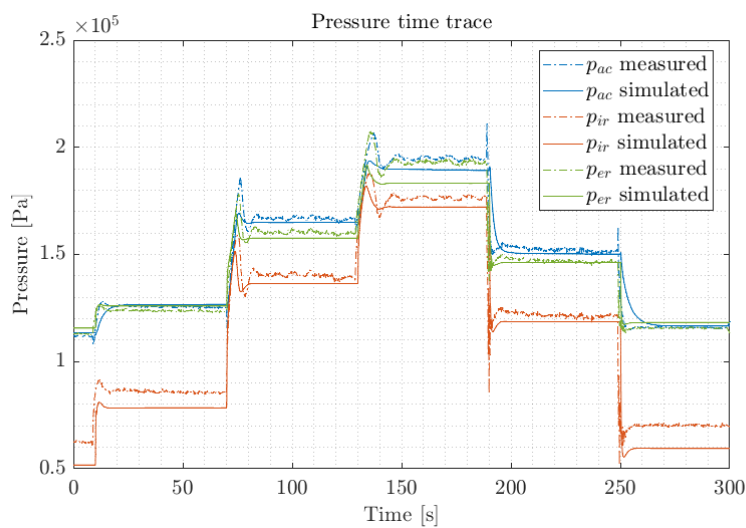


Figure 4: Pressure time trace of the volume elements

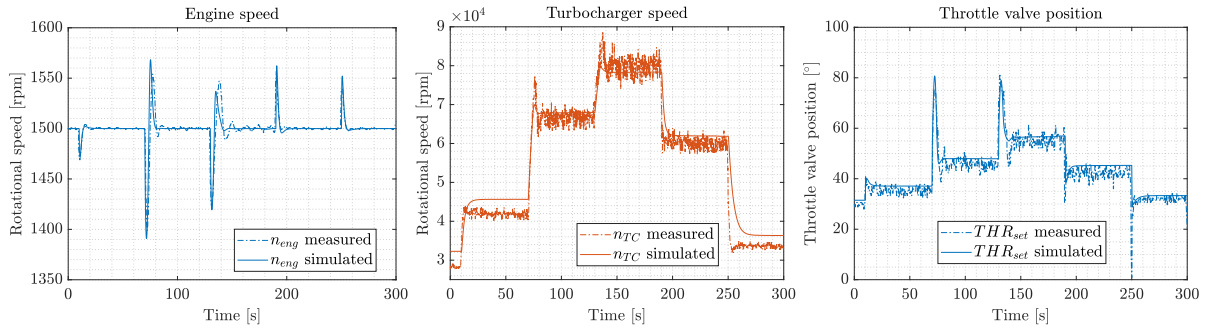


Figure 5: Time traces engine parameters validation

4.1 Pulsed loads with decreasing load ramp up time

The first load profile represents pulsed loads from 20 to 100% of MCR load with decreasing load ramp up time, ranging from 30s to 20s and subsequently 15s to 8s in steps of 1s, see Figure 6. The results demonstrate that the gas engine is able to follow the requested pulse load up to a load ramp up rate of $36kW/s$ ($90 - 450kW$ in 10s). However, the engine speed shows an increasing deviation from the set point resulting in lower dips and higher overshoots. For a higher ramp up rate the throttle fully opens (82°) but the turbocharger is not able to follow and the charge air pressure starts to lag. Consequently the delivered torque and power are insufficient and the engine speed drops. Due to the reduced mass flow in the exhaust, the turbine of the turbocharger produces less torque and the turbocharger speed levels off as with a cascading effect on charge air pressure, delivered engine torque and resulting engine speed. A new balance is found at an engine speed of $1140rpm$. According to NATO STANAG 1008 for Quality Power Supply (QPS) a maximum deviation of 4% from the grid frequency is allowed during transient operations, see Table 4, limiting the load ramp up rate to $33kW/s$ ($90 - 450kW$ in 11s).

4.2 Varying step loads

The second load profile examined contains several step loads between 0 and 100% of MCR load, see Figure 7 for the load profile and the results. From the results, we conclude that the requested load steps are slightly too high

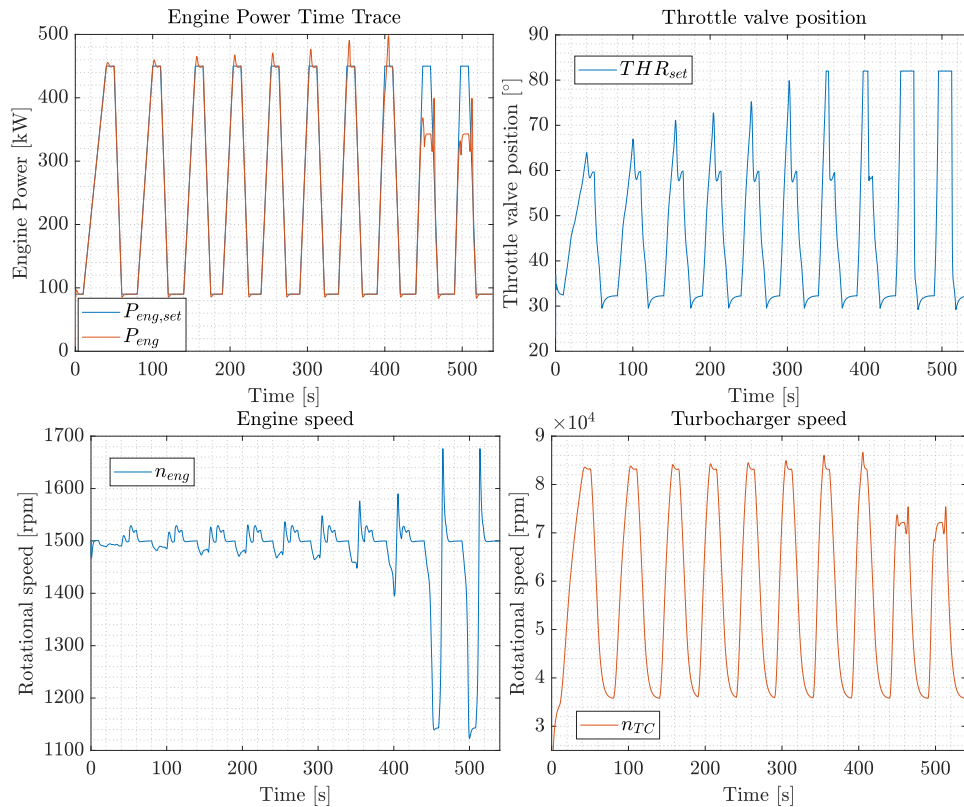


Figure 6: Results simulation experiment 1: Pulsed loads 20–100% MCR

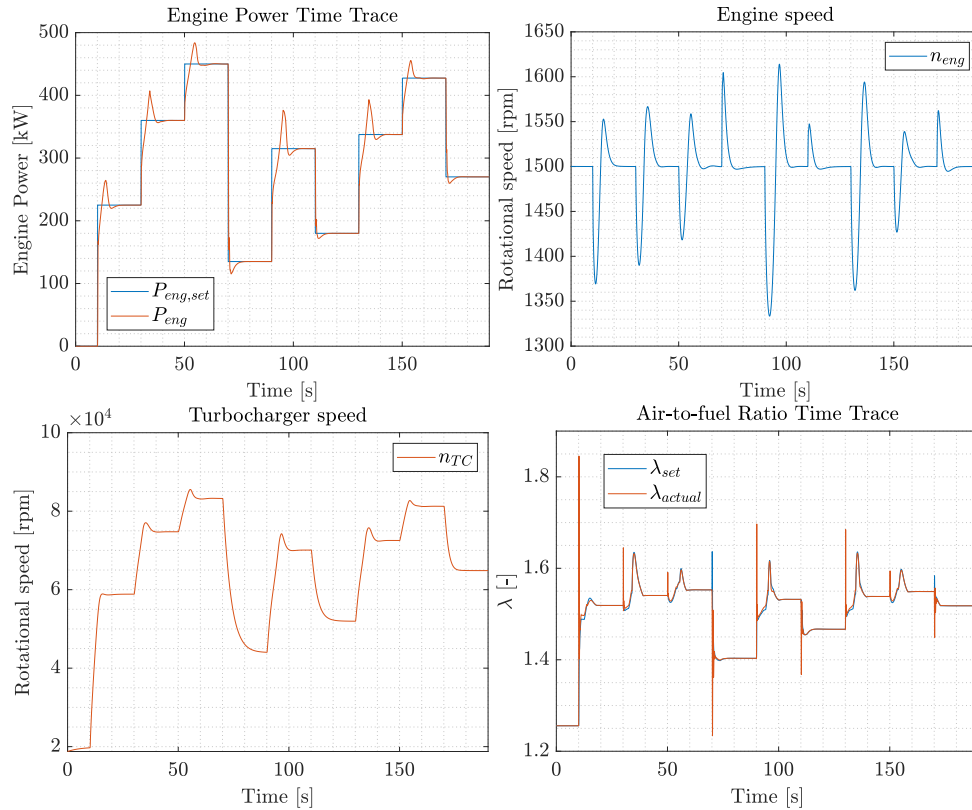


Figure 7: Results simulation experiment 2: Varying step loads

for the engine, since the engine cannot follow the load profile exactly and the engine speed deviates more than 10% from the setpoint. However, the results for the air excess ratio are more interesting. Diesel engines suffer from low air excess ratios resulting in incomplete combustion and emission of soot during sharp load increases due to the supply of fresh air by the air path lagging the fast supply of fuel by the fuel pump. For a gas engine this could result in auto-ignition of the fuel and thus severe knocking of the engine. With single point injection of fuel before the compressor in this particular type of engine fresh air and fuel supply are simultaneously influenced by the gas path and turbocharger dynamics. During the initial phase of the load increase and with opening of the throttle valve the mass flow and charge air pressure to the cylinder increase while additional fuel supplied has to travel through the compressor first. This results in the air excess ratio spiking rather than dipping during load increases and thus reduces the risk of engine knocking. Decreasing the load results in the opposite effect with the air excess ratio dipping. Due to decreasing in-cylinder temperatures and pressures the risk of engine knocking nevertheless decreases.

4.3 Load profile rail gun

The third load profile represents the load demand of an electromagnetic railgun firing three shots at the rate of one shot per 6s and an initial charge time of 17.5s according to [52]. The load profile and the results are given in Figure 8. Results of this simulation experiment show that the engine is able to follow the load increase during the charging phase before and between the shots well but struggles to follow the peak load during firing of the projectile (at 22.5s, 28.5s and 34.5s). Compared to the gas turbine generator used by Whitelegg et al. [52], the gas engine's inertia is preventing the engine from following the exact shape of the peak resulting in delivering just 87% of the requested power for the first shot and 81% of the requested power for the second shot. This results in an energy deficit of about 560kJ for the first shot and 760kJ for the second shot and could require the use of super

Table 4: QPS Frequency characteristics according to STANAG 1008 [51]

| Characteristics | Tolerance | Transient Tolerance | Worst Case Excursion |
|-----------------|-----------|---------------------|----------------------|
| Frequency 60Hz | $\pm 3\%$ | $\pm 4\%$ | $\pm 5.5\%$ |
| Recovery time | - | 2s | 2s |

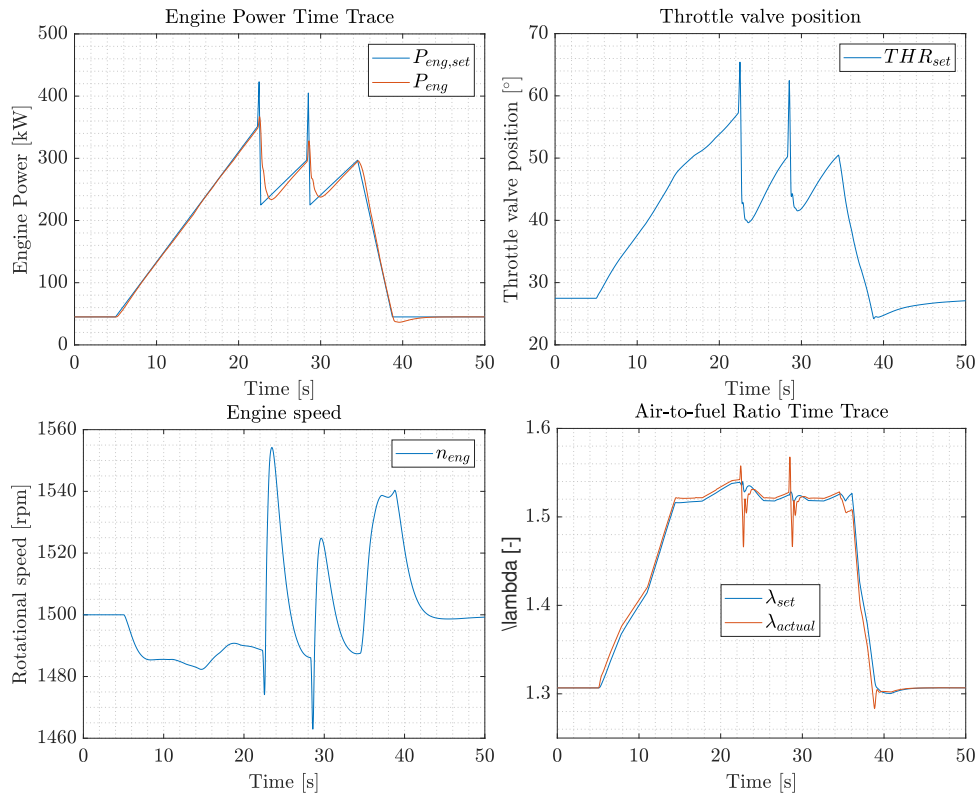


Figure 8: Results simulation experiment 3: Load profile rail gun

capacitors to supply additional energy. Furthermore, we conclude that the implemented controller is performing well during a load increase but less after reaching the requested power or during a load decrease resulting in a large overshoot in engine speed. With a maximum deviation of the engine speed of 3.5% and a quick recovery, the engine is able to fulfill the requirements of NATO STANAG 1008, see Table 4.

5 Conclusions and recommendations

Current research on modelling of marine internal combustion engines running on alternative fuel focuses on sophisticated crank angle models with multiple zone combustion models or even 3D CFD models to determine the performance of dual-fuel engines as accurately as possible, since these engines promise the highest efficiencies. On the contrary, this paper provides two interesting results with a simpler modelling approach with a mean value first principle model of a spark ignited gas engine. With the available data limited to the operating and maintenance manual and one measurement run of 4 step loads and a measurement duration of 230s, we could calibrate the derived simulation model to produce sufficiently accurate results of the steady state and transient performance for a variety of engine parameters. While it is hard to limit the absolute error due to measurement variances and time offsets during the transient phases, we achieved an average error below 5% for most of the engine parameters, while the model was running the model significantly faster than real time. More importantly, the model is able to predict the transient performance well enough to comment on the impact of injection strategy, combustion mode and control strategy on the performance of the engine. Therefore, the model is suitable for investigating dynamic operating profiles and control oriented modelling approaches.

Subsequently, the model could be used to examine propulsion plant behaviour and evaluate engine and system control strategies in real-time. From the simulation experiments, we concluded that the transient performance is limited by the inertia of gas path in general and the turbocharger in particular. Moreover, the injection strategy with single point injection of fuel before the compressor in combination with the premixed combustion mode significantly reduces the risk of engine knocking during load steps compared to the direct injection of gas, because fresh air and fuel are influenced by the gas path dynamics at the same time and are well mixed when entering the cylinder. However, the limitations in load acceptance due to the gas path dynamics remain. With this in mind, the application of spark ignited combustion engines for marine purposes should be reconsidered in case transient performance is of higher importance than efficiency.

From the experiments several recommendations can be made. First, the engine is limited to operation on the generator line with a constant engine speed with the current experimental set up. To investigate the transient per-

formance over the complete engine envelope, to represent state-of-the-art DC architectures with variable speed generators, the experimental set up should facilitate variable engine speed as well. Secondly, the proposed model was set up to investigate transient performance on methanol as a fuel as well. The current experimental set up will be extended with a port fuel injection system for methanol. This will require adaptations to the developed simulation model approach, since the dynamics of the injection of liquid methanol close to the cylinder and evaporation of the fuel will significantly deviate from the currently implemented injection dynamics. Therefore, in future, we aim to use these models to investigate the dynamic performance and advanced control approaches for methanol generators in a DC architecture with variable speed engine operation, thus contributing to both the use of alternative fuel and the improvement of power system efficiency.

References

- [1] Directoraat-Generaal Beleid / Directie Materieel Vastgoed En Duurzaamheid, ROADMAP ENERGIETRANSITIE OPERATIONEEL MATERIEEL, Technical Report, MINISTERIE VAN DEFENSIE, 2022.
- [2] R. McGill, W. Remley, K. Winther, Alternative Fuels for Marine Applications: A Report from the IEA Advanced Motor Fuels Implementing Agreement., Technical Report, International Energy Agency - Advanced Motor Fuels, 2013.
- [3] S. Verhelst, J. W. Turner, L. Sileghem, J. Vancoillie, Methanol as a fuel for internal combustion engines, *Progress in Energy and Combustion Science* 70 (2019) 43–88.
- [4] B. Mestemaker, M. G. Castro, H. van den Heuvel, K. Visser, Dynamic simulation of a vessel drive system with dual fuel engines and energy storage, *Energy* 194 (2020) 116792.
- [5] CIMAC WG17, Transient response behaviour of gas engines, CIMAC Technical Report (2011).
- [6] J. Vollbrandt, Improving the maneuvering performance of diesel hybrid propulsion plants for fast naval combatant, 2016.
- [7] R. Pawling, L. Farrier, R. Bucknall, The advanced technology corvette-railgun (atk-r) design study-future weapons and small ship power systems, in: *Proceedings of the International Naval Engineering Conference and Exhibition (INEC)*, IMarEST, 2018, pp. 1–17.
- [8] T. Korakianitis, A. Namasivayam, R. Crookes, Natural-gas fueled spark-ignition (si) and compression-ignition (ci) engine performance and emissions, *Progress in energy and combustion science* 37 (2011) 89–112.
- [9] J. S. Katsanis, E. G. Pariotis, R. G. Papagiannakis, Natural gas combustion in marine compression ignition and spark ignition engines: A technological, environmental and economic evaluation, in: *Annual Meeting of Marine Technology 2017*, 2017, pp. 1–13.
- [10] H. M. Cho, B.-Q. He, Spark ignition natural gas engines—a review, *Energy conversion and management* 48 (2007) 608–618.
- [11] R. Geertsma, J. Vollbrandt, R. Negenborn, K. Visser, H. Hopman, A quantitative comparison of hybrid diesel-electric and gas-turbine-electric propulsion for future frigates, in: *2017 IEEE Electric Ship Technologies Symposium (ESTS)*, IEEE, 2017, pp. 451–458.
- [12] C. Sui, P. de Vos, D. Stapersma, K. Visser, H. Hopman, Y. Ding, Mean value first principle engine model for predicting dynamic behaviour of two-stroke marine diesel engine in various ship propulsion operations, *International Journal of Naval Architecture and Ocean Engineering* 14 (2022) 100432.
- [13] R. Geertsma, K. Visser, R. Negenborn, Adaptive pitch control for ships with diesel mechanical and hybrid propulsion, *Applied energy* 228 (2018) 2490–2509.
- [14] A. Vrijdag, Control of Propeller Cavitation in Operational Conditions, Ph.D. thesis, Delft University of Technology, 2009.
- [15] M. S. Cellek, A. Pınarbaşı, Investigations on performance and emission characteristics of an industrial low swirl burner while burning natural gas, methane, hydrogen-enriched natural gas and hydrogen as fuels, *International Journal of Hydrogen Energy* 43 (2018) 1194–1207.
- [16] H. Wang, H. Gan, G. Theotokatos, Parametric investigation of pre-injection on the combustion, knocking and emissions behaviour of a large marine four-stroke dual-fuel engine, *Fuel* 281 (2020) 118744.
- [17] J. Zareei, A. Rohani, W. M. F. W. Mahmood, Simulation of a hydrogen/natural gas engine and modelling of engine operating parameters, *International Journal of Hydrogen Energy* 43 (2018) 11639–11651.
- [18] L. Xiang, G. Theotokatos, Y. Ding, Parametric investigation on the performance-emissions trade-off and knocking occurrence of dual fuel engines using cfd, *Fuel* 340 (2023) 127535.
- [19] J. B. Heywood, *Internal combustion engine fundamentals*, McGraw-Hill Education, 2018.
- [20] F. Maroteaux, C. Saad, F. Aubertin, Development and validation of double and single wiebe function for multi-injection mode diesel engine combustion modelling for hardware-in-the-loop applications, *Energy Conversion and Management* 105 (2015) 630–641.
- [21] M. Tadros, M. Ventura, C. G. Soares, Simulation of the performance of marine genset based on double-wiebe function, in: *Sustainable Development and Innovations in Marine Technologies*, CRC Press, 2019, pp. 292–299.
- [22] H. Sapra, M. Godjevac, P. De Vos, W. Van Sluijs, Y. Linden, K. Visser, Hydrogen-natural gas combustion in a marine lean-burn si engine: A comparative analysis of seiliger and double wiebe function-based zero-dimensional modelling, *Energy Conversion and Management* 207 (2020) 112494.
- [23] S. Stoumpos, G. Theotokatos, E. Boulougouris, D. Vassalos, I. Lazakis, G. Livanos, Marine dual fuel engine modelling and parametric investigation of engine settings effect on performance-emissions trade-offs, *Ocean Engineering* 157 (2018) 376–386.
- [24] S. Xu, D. Anderson, M. Hoffman, R. Prucka, Z. Filipi, A phenomenological combustion analysis of a dual-fuel natural-

- gas diesel engine, *Proceedings of the Institution of Mechanical Engineers, Part D: Journal of Automobile Engineering* 231 (2017) 66–83.
- [25] A. Chevalier, M. Müller, E. Hendricks, On the validity of mean value engine models during transient operation, *SAE transactions* (2000) 1571–1592.
- [26] L. Guzzella, C. Onder, *Introduction to modeling and control of internal combustion engine systems*, Springer Science & Business Media, 2009.
- [27] E. Hendricks, A. Chevalier, M. Jensen, S. C. Sorenson, D. Trumpy, J. Asik, Modelling of the intake manifold filling dynamics, *SAE transactions* (1996) 122–146.
- [28] J. Reiß, C. Stürzebecher, C. Bohn, F. Märzke, R. Frase, A diesel engine model including exhaust flap, intake throttle, lp-egr and vgt. part i: system modeling, *IFAC-PapersOnLine* 48 (2015) 52–59.
- [29] M. Altosole, G. Benvenuto, U. Campora, M. Figari, et al., Dynamic performance simulation of a naval propulsion system, in: *Summer Computer Simulation Conference*, 2004, pp. 243–248.
- [30] G. Theotokatos, N. Kyrtatos, Investigation of a large high-speed diesel engine transient behavior including compressor surging and emergency shutdown, *J. Eng. Gas Turbines Power* 125 (2003) 580–589.
- [31] G. Theotokatos, S. Stoumpos, V. Bolbot, E. Boulougouris, Simulation-based investigation of a marine dual-fuel engine, *Journal of Marine Engineering & Technology* 19 (2020) 5–16.
- [32] S. Stoumpos, G. Theotokatos, C. Mavrelou, E. Boulougouris, Towards marine dual fuel engines digital twins—integrated modelling of thermodynamic processes and control system functions, *Journal of Marine Science and Engineering* 8 (2020) 200.
- [33] S. Tavakoli, S. Saettone, S. Steen, P. Andersen, J. Schramm, E. Pedersen, Modeling and analysis of performance and emissions of marine lean-burn natural gas engine propulsion in waves, *Applied Energy* 279 (2020) 115904.
- [34] L. Eriksson, L. Nielsen, J. Brugrd, J. Bergström, F. Pettersson, P. Andersson, Modeling of a turbocharged si engine, *Annual reviews in control* 26 (2002) 129–137.
- [35] C. H. Onder, M. Betschart, T. S. Auckenthaler, L. Guzzella, Modelling and control of an active throttle for si engines, *IFAC Proceedings Volumes* 37 (2004) 155–160.
- [36] J. Wahlström, L. Eriksson, Modeling of a diesel engine with intake throttle, vgt, and egr, 2010.
- [37] M. Seiliger, *Die Hochleistungs-Dieselmotoren*, J. Springer, 1926.
- [38] R. Geertsma, R. Negenborn, K. Visser, M. Loonstijn, J. Hopman, Pitch control for ships with diesel mechanical and hybrid propulsion: Modelling, validation and performance quantification, *Applied energy* 206 (2017) 1609–1631.
- [39] P. Schulten, The interaction between diesel engines, ship and propellers during manoeuvring, Ph.D. thesis, Delft University of Technology, 2005.
- [40] J. H. Horlock, D. Winterbone, *The thermodynamics and gas dynamics of internal-combustion engines. Volume II*, New York, NY: Oxford University Press, 1986.
- [41] M. Casey, C. Robinson, A method to estimate the performance map of a centrifugal compressor stage, *Journal of turbomachinery* 135 (2013) 021034.
- [42] J.-P. Jensen, A. Kristensen, S. C. Sorenson, N. Houbak, E. Hendricks, Mean value modeling of a small turbocharged diesel engine, Technical Report, SAE Technical Paper, 1991.
- [43] P. Moraal, I. Kolmanovsky, Turbocharger modeling for automotive control applications, Technical Report, SAE Technical Paper, 1999.
- [44] P. Cat, *Operation and Maintenance Manual, 3500B Series II and 3500C Marine Auxiliary Engines*, Caterpillar, 2008.
- [45] Diesel Levante srl, *Turbochargers Catalogue*, Diesel Levante srl, 2014.
- [46] H. Sapra, Y. Linden, W. van Sluijs, M. Godjevac, K. Visser, Experimental investigations of performance variations in marine hydrogen-natural gas engines, in: *Cimac Congress*, volume 2019, 2019, pp. 1–17.
- [47] J. Bosklopper, H. Sapra, R. van de Ketterij, W. van Sluijs, C. Bekdemir, P. de Vos, K. Visser, Experimental study on a retrofitted marine size spark-ignition engine running on port-injected 100% methanol, *INEC 2020*, Delft (2020).
- [48] R. Geertsma, M. Krijgsman, *Alternative fuels and power systems to reduce environmental impact of support vessels*, Delft University of Technology (2019).
- [49] W. Astley, A. Grasman, D. Stroeve, Exploring the impact of methanol as an alternative, cleaner fuel for the auxiliary and support vessels within the rnl, *Proc. INEC* (2020).
- [50] Caterpillar, *G3508 LE Gas Petroleum Engine Specifications*, Caterpillar, 2010.
- [51] NATO, *NATO - STANAG 1008: CHARACTERISTICS OF SHIPBOARD 440V/230V/115V 60Hz, 440V/115V 400Hz and 24/28VDC ELECTRICAL POWER SYSTEMS IN WARSHIPS OF THE NATO NAVIES*, Technical Report, North Atlantic Treaty Organization (NATO), 2021.
- [52] I. Whitelegg, R. Bucknall, B. Thorp, On electric warship power system performance when meeting the energy requirements of electromagnetic railguns, *Journal of Marine Engineering & Technology* 14 (2015) 85–102.

A Appendix: Model parameters

Table 5: Model parameters

| Engine Parameter | Value |
|---|-------------------------------------|
| Nominal power $P_{e,nom} = 90\%P_{e,rated}$ | 450kW |
| Nominal specific fuel consumption (NG) $m_{bsfc,nom}$ | 290.1g/kWh |
| Geometric compression ratio r_c | 12 |
| Temperature of the inlet receiver T_{ir} | 37°C |
| Closed in-cylinder parameters | Value |
| Nominal heat release efficiency $\eta_{q,nom}$ | 0.75 |
| Heat release gradient X_q | 0.21 |
| Cylinder volume at state 1 V_1 | 0.0047m ³ |
| Nominal pressure at state 1 $p_{1,nom}$ | 1.975e ⁵ Pa |
| Nominal maximum cylinder pressure $p_{max,nom}$ | 69e ⁵ Pa |
| Nominal mechanical efficiency $\eta_{m,nom}$ | 0.885 |
| Heat release fraction isochoric combustion X_{cv} | 0.07 |
| Heat release fraction isothermal combustion X_{ct} | 0.42 |
| Nominal Seiliger parameter a | 1.2185 |
| Nominal Seiliger parameter b | 1.4422 |
| Nominal Seiliger parameter c | 2.9196 |
| Throttle valve parameters | Value |
| Diameter throttle pipe D_{THR} | 0.104m |
| Diameter axis throttle valve d_{THR} | 0.01m |
| Discharge coefficient throttle valve reference | 30° – 60° – 90° |
| Discharge coefficient throttle valve C_D | 0.7 – 0.79 – 0.99 |
| Turbocharger parameters | Value |
| Rotational inertia turbocharger J_{TC} | 0.0015kg * m ² |
| Mechanical efficiency reference | 10 – 30 – 60 – 90e ⁴ rpm |
| Mechanical efficiency $\eta_{m,TC}$ | 0.99 – 0.98 – 0.96 – 0.90 |
| Air and exhaust gas properties | Value |
| Ambient pressure p_a | 1.02e ⁵ Pa |
| Ambient temperature T_a | 35.7°C |
| Gas constant of air R_a | 287J/kgK |
| Specific heat at constant volume of air $c_{v,a}$ | 717.5J/kgK |
| Specific heat at const. pressure of air $c_{p,a}$ | 1004.5J/kgK |
| Specific heat at const. pressure of exhaust gas $c_{p,g}$ | 1094J/kgK |
| Isentropic index of air κ_a | 1.4 |
| Isentropic index of exhaust gas κ_g | 1.3556 |
| Polytropic exponent for expansion n_{exp} | 1.38 |
| Polytropic exponent for blowdown n_{bl} | 1.38 |
| Fuel properties | Value |
| Lower heating value fuel h^L | 38120kJ/kg |
| Stoichiometric gravimetric air to fuel ratio σ_g | 14.65 |
| Controller properties | Value |
| Proportional gain K_P | 3.2 |
| Integral gain K_I | 0.28 |
| Derivative gain K_D | 1.0 |